Published in final edited form as:
Mol Cancer Res. 2011 February ; 9(2): 206–214. doi:10.1158/1541-7786.MCR-10-0451.

The homologous recombination protein RAD51D mediates the processing of 6-thioguanine lesions downstream of mismatch repair

Preeti Rajesh, **Alexandra Litvinchuk**[#], **Douglas L. Pittman**[*], and **Michael D. Wyatt**[*]
Department of Pharmaceutical and Biomedical Sciences, South Carolina College of Pharmacy, University of South Carolina, Columbia SC 29208

Abstract

Thiopurines are extensively used as immunosuppressants and in the treatment of childhood cancers, even though there is concern about therapy-induced leukemias and myelodysplastic syndromes resulting from thiopurine use. Following metabolic activation, thiopurines are incorporated into DNA and invoke mismatch repair (MMR). Recognition of 6-thioguanine (6-thioG) in DNA by key MMR proteins results in cell death rather than repair. There are suggestions that homologous recombination (HR) is involved downstream of MMR following thiopurine treatment, but the precise role of HR is poorly understood. In this study, we demonstrate that cells deficient in RAD51D (a RAD51 paralog) are extremely sensitive to 6-thioG. This sensitivity is almost completely rescued by the deletion of *Mlh1*, which suggests that HR is involved in the repair of the 6-thioG induced recombinogenic lesions generated by MMR. Furthermore, 6-thioG induces chromosome aberrations in the *Rad51d*-deficient cells. Interestingly, *Rad51d*-deficient cells show a striking increase in the frequency of triradial and quadriradial chromosomes in response to 6-thioG. The presence of these chromatid exchange type aberrations indicate that the deficiency in RAD51D-dependent HR results in profound chromosomal damage precipitated by the processing of 6-thioG by MMR. The radials are notable as an important source of chromosomal translocations, which are the most common class of mutations found in hematological malignancies. This study thus suggests that HR-insufficiency could be a potential risk factor for the development of secondary cancers that result from long-term use of thiopurines in patients.

Keywords

Mismatch repair; Homologous recombination; RAD51D; MLH1; Thiopurines

Introduction

Antimetabolite thiopurines are extensively used as immunosuppressants and in the treatment of childhood cancers. However, there is increasing concern about therapy-induced leukemias and myelodysplastic syndromes in patients treated with thiopurines, particularly maintenance therapies. For example, the relative risk of developing leukemia is 5.3 for heart

[*]To whom correspondence should be addressed. Department of Pharmaceutical and Biomedical Sciences, South Carolina College of Pharmacy, University of South Carolina, 715 Sumter Street, Columbia SC 29208 Tel: 1 803 777 0856; fax: 1 803 777 8356. wyatt@sccp.sc.edu Tel: 1 803 777 7715; fax: 1 803 777 8356. pittman@sccp.sc.edu.
[#]Current address: Department of Radiation Oncology, Health Science Center, University of Florida, Gainesville FL 32610

and/or lung transplant patients (1). Data from a large French cohort of patients (19,486) with inflammatory bowel disease identified a relative risk of developing lymphoproliferative disorders as 5.2 for patients who were treated with thiopurines compared to those who were not (2). Despite the success stories treating childhood leukemias with thiopurines as part of the regimen, there is a clear risk of secondary neoplasms associated with the duration and intensity of maintenance therapy (3).

Although DNA is acknowledged as the ultimate target, the molecular mechanisms by which thiopurines exert their antiproliferative effects via DNA damage are poorly understood. Thiopurines are metabolized to form 6-thioguanine (6-thioG), which is ultimately misincorporated into DNA opposite thymine (1). The cytotoxic DNA damage that 6-thioG induces is intriguing in that it invokes two DNA repair responses, mismatch repair (MMR) and homologous recombination (HR), with differing consequences. Biochemically, base:base mismatches are recognized by two heterodimeric MMR protein complexes, MSH2:MSH6 (also known as MutSα) and MLH1:PMS2 (also known as MutLα), which recruit exonuclease 1 (Exo1). Processing of 6-thioG:T and the structurally similar O^6-methyl guanine (O^6-meG) adduct by MutSα, MutLα, and Exo1 does not lead to repair, but instead triggers cell death (4,5). Therefore, loss of MMR by genetic or epigenetic means can promote a 'tolerance' to DNA damage and resistance to DNA damaging agents (6-8). There has been debate whether the induction of apoptosis results from MMR's 'futile' attempt at repair, or the involvement of MMR proteins in DNA damage checkpoint signaling. Data from studying mutants of MSH2 and MSH6 suggested that the mismatch correction and damage-sensing functions of MMR are distinct (9,10). Yet, more recent papers clearly implicate the involvement of the nuclease function of Exo1 downstream of MutSα/MutLα, because Exo1-deficient mice and cells, including cells expressing a nuclease-deficient Exo1, are resistant to killing by 6-thioG and agents that cause O^6-meG (4,5).

The role of HR in the cellular response to thiopurines is poorly understood, but there is cytogenetic and genetic evidence that HR is involved in processing 6-thioG and O^6-meG lesions, regardless of the precise damage signaling and/or futile cycling roles of MMR. For example, 6-thioG induces sister chromatid exchanges (SCEs), a strong indicator of HR events, that are dependent on the presence of functional MMR (11). We recently reported the generation of a unique mouse model combining MMR and HR defects by deletion of *Mlh1* and *Rad51d* (12). RAD51D is a member of the Rad51-protein family that plays an important role in HR, and has been identified to interact as part of a complex with MSH2 in a proteomics screen of RAD51D interacting partners (13). We demonstrated that the sensitivity of *Rad51d*-deficient cells to MNNG, an alkylating agent that causes O^6-meG, was partially dependent on the presence of MMR. Loss of *Mlh1* not only alleviated sensitivity of *Rad51d*-deficient cells to MNNG but also reduced γ-H2AX induction, G2/M cell cycle arrest and apoptosis. In addition to RAD51D, other HR proteins including XRCC2, XRCC3 and BRCA2 have been implicated in protection against O^6-meG lesions (14,15). Cells deficient in the FancG protein are sensitized to 6-thioG (16), and recently, it was reported that BRCA2 deficient cells are sensitive to 6-thioG (17), thus implicating RAD51-associated HR in the cellular response to thiopurines.

In this study, we examined the role of RAD51D in repair of 6-thioG induced DNA damage and find that HR is indeed required in the cellular response to 6-thioG induced damage downstream of MMR. *Rad51d*-deficient MEFs are hypersensitive to 6-thioG and this sensitivity is almost completely dependent on the presence of MMR. *Rad51d*-deficient cells show a heightened G2 arrest accompanied by an increase in the aneuploid cell population and multinucleation. In addition, there is a substantial increase in the chromosomal aberrations, especially radials in the *Rad51d*-deficient cells upon 6-thioG treatment. These

findings have implications for understanding the mechanisms of therapy-induced cancers caused by therapeutic thiopurines.

Materials and methods

Cell Lines

Mouse embryonic fibroblast (MEF) cell lines *Rad51d*$^{+/+}$*Trp53*$^{-/-}$, *Rad51d*$^{-/-}$*Trp53*$^{-/-}$, *Rad51d*$^{-/-}$*Trp53*$^{-/-}$ *Mlh1*$^{-/-}$ and *Mlh1*$^{-/-}$*Trp53*$^{-/-}$ were generated and characterized as described previously (12). Because *Rad51d*$^{-/-}$ MEFs with wild-type p53 fail to proliferate, all comparisons between MLH1 and RAD51D status were made with *Trp53*$^{-/-}$ cells. The cell lines were cultured in Dulbecco's modified Eagle's medium (DMEM) (Cellgro Mediatech, VA, USA) supplemented with 10% Newborn Calf Serum (NCS), 2 mM Glutamine and 100 U/ml penicillin-streptomycin (Hyclone, UT, USA).

Colony Survival Assays

For colony survival assays, MEFs were seeded onto 100 mm dishes at 800 cells per plate in DMEM (Cellgro) supplemented with 10% Fetal Bovine Serum, 2 mM Glutamine and 100 U/ml penicillin-streptomycin (Hyclone). Cells were treated with 6-thioG (Sigma-Aldrich, MO, USA) at the indicated concentrations. After 24 h treatment, 6-thioG was removed and fresh medium was added. During the experiment, the medium was replaced once after 5 days. Cells were grown for 8 to 10 days, fixed with 100% methanol and stained with Giemsa (Sigma-Aldrich). Colonies containing 50 or more cells were counted. Three independent experiments were performed and each experiment performed in triplicates. Error bars represent the standard error of the mean. The LC_{50} values were calculated from a semi-log plot generated by non-linear regression analysis using GraphPad Prism 4.0 software (GraphPad Software, Inc. CA, USA).

Cell Cycle Analysis

For cell cycle analysis, 1.0×10^5 cells were seeded onto 100 mm dishes, and the medium containing 0.1 μM 6-thioG was added to the treatment plates 42 h after seeding. The medium was replaced 6 h post treatment with drug free medium. At the indicated time points post treatment, all cells were collected, washed with phosphate-buffered saline (PBS), and gently resuspended in propidium iodide (50 μg/ml) staining solution containing 4 mM sodium citrate (pH 7.8), 30 units/ml RNase A (Sigma), and 0.1% Triton X-100. After an incubation period of 10 min at 37 °C, NaCl was added to a final concentration of 0.15 M (18). Cell cycle analyses were performed using a Beckman Coulter FC 500 cytometer (Beckman Coulter, CA, USA) and data was quantified using ModFit LT software version 3.1 (Verity Software House, ME, USA).

Mitotic Index

Cells were treated with 0.1 μM 6-thioG for 6 h, then incubated in medium containing 200 ng/ml nocodazole for 6 h before harvesting at 48 h and 72 h time points post treatment. The cells were fixed in 70% ethanol overnight (-20 °C) and then permeabilized with 0.25% Triton X-100 and stained with phospho-histone H3 antibody Alexa fluor 488 conjugate (Cell Signaling, MA, USA) followed by propidium iodide (10 μg/ml PI and 100 μg/ml RNaseA in PBS) staining. The cells were then analyzed using a Beckman Coulter FC 500 cytometer (Beckman Coulter) and data was quantified using CXP analysis software (Beckman Coulter).

Metaphase spreads and nuclear phenotypes

Giemsa stained metaphase spreads were prepared as described (19). In brief, cells were treated with 0.1 μM 6-thioG for 6 h and mitotic cells were harvested at 24 h, 48 h and 72 h time points following a three-hour incubation with 20 ng/ml colcemid (Roche Applied Science, IN, USA). The cells were incubated in hypotonic solution [5% (v/v) NCS, 2 mg/ml KCl and 2 mg/ml sodium citrate in distilled water] for 15 min at 37 °C twice followed by two rounds of fixation in fresh ice-cold Carnoy's fixative [3:1 (v/v) mixture of methanol and acetic acid]. To prepare chromosome spreads, fixed cells were dropped onto the slides; air dried, stained with 4% Giemsa (Sigma), washed in water and mounted using Permount© (Thermo Fisher Scientific, MA, USA). The slides were observed on a Nikon Eclipse E600 Microscope using 100 × objective, and the images were captured using a Q-imaging CCD camera. Chromosomal aberrations were scored from a minimum of 1000 chromosomes.

Sister Chromatid Exchange Analysis

Sister Chromatid Exchange analysis was performed as described (19). In brief, 5×10^5 cells were seeded onto 100-mm dishes and 24 h later medium containing 0.1 μM 6-thioG and 10 μM Bromodeoxyuridine (BrdU) (Sigma-Aldrich) was added to the cells. After 6 h of 6-thioG treatment, fresh medium containing only 10 μM BrdU was added. The cells were harvested 48 h later following 3 h incubation with 20 ng/ml colcemid (Roche), and metaphase spreads were prepared as described above. The spreads were then differentially stained by incubation in 10 μg/ml Hoechst in 1X Sorenson's buffer, rinsed in 2X SSC, exposed to black light for 45 min at 65° C, and subsequently rinsed with 1X Sorenson's buffer. Staining, mounting, and observations were performed as described for the metaphase spreads.

Immunofluorescence

The cells were plated at the density of 5000 cells per coverslip, 24 h prior to treatment with 0.1 μM 6-thioguanine. The medium was changed 6 h post treatment. After the treatment, the coverslips were washed with PBS, incubated for 30 sec in microtubule stabilization buffer (130 mM Hepes; 4.2 mM $MgCl_2$; 10 mM EGTA, pH 6.9). The cells were fixed with 4% formaldehyde (Thermo Fisher Scientific, MA, USA) and permeabilized with 0.2% Triton X-100. Fixed cells were incubated with β-tubulin antibody (Abcam, MA, USA) overnight at 4° C and alexafluor 488 conjugated anti-rabbit secondary IgG (Molecular Probes, CA, USA) for 1 h at room temperature to visualize microtubules. Nuclei were stained with DAPI, and the cells were mounted. The coverslips were examined on an Olympus microscope (IX81) using a 40x objective and the images were captured using Hamamatsu OrcaR2 camera, and at least 500 cells were counted per sample.

Statistical Analysis

Calculations of the mean, standard deviation and standard error were performed using Microsoft Excel. Statistical analysis for comparison of each set of experimental means was performed using Graphpad Instat 3.0 (Graphpad Software Inc., La Jolla, CA). Statistical analysis of proportions was performed using the Sigmaplot 11 (Systat Software Inc., San Jose, CA).

Results

Absence of RAD51D enhances the sensitivity of MMR-proficient cells to 6-ThioG

We previously developed a *Rad51d* and *Mlh1* deficient MEF cell line to study the combined defects of MMR and HR (12). In this study, we first confirmed that absence of *Mlh1* alleviated the sensitivity of *Rad51d*-proficient cells to 6-thioG, by 10.1-fold (Fig. 1A),

which agreed with previous studies (20). Next, the role of RAD51D in response to 6-thioG in a wild-type mismatch repair background was evaluated. *Rad51d*$^{-/-}$*Mlh1*$^{+/+}$ cells were approximately 4.9-fold more sensitive to 6-thioG, with an LC_{50} value of 0.065 μM compared to 0.32 μM for *Rad51d*$^{+/+}$*Mlh1*$^{+/+}$ cells (Fig. 1B). The next comparison was to see whether loss of MMR alleviated the sensitivity of the HR deficient cells. Indeed, the *Rad51d*$^{-/-}$*Mlh1*$^{-/-}$ cells were dramatically resistant compared to *Rad51d*$^{-/-}$*Mlh1*$^{+/+}$ cells, by 36.4-fold (Fig. 1C). In other words, when one compares sensitivity in the *Mlh1*-deficient background, the *Rad51d*-deficient cells were only 1.4-fold more sensitive to 6-thioG than *Rad51d*-proficient cells, with an LC_{50} value of 2.38 μM compared to 3.23 μM (Supplementary Fig. S1). This compellingly shows that the hypersensitivity of HR deficient cells is downstream of MMR and highly dependent on functional MMR. We also observed an increased induction of the sub-G_1 population in the *Rad51d*-deficient cells in response to 6-thioG, indicating the role of RAD51D in repairing lesions that otherwise induce apoptosis (Supplementary Fig. S2B).

6-ThioG-induced G2 arrest is heightened in Rad51d-deficient cells

Previous studies have shown that 6-thioG induces a G2 arrest in MMR proficient cells (21). Here, we examined the influence of HR on the 6-thioG induced G2 arrest by examining cell cycle progression in the *Rad51d*$^{+/+}$*Mlh1*$^{+/+}$, *Rad51d*$^{-/-}$*Mlh1*$^{+/+}$ and *Rad51d*$^{-/-}$*Mlh1*$^{-/-}$ cell lines. Following treatment with 0.1 μM 6-thioG, an increase in the 4N population was observed in both *Rad51d*$^{+/+}$*Mlh1*$^{+/+}$ and *Rad51d*$^{-/-}$*Mlh1*$^{+/+}$ cell lines 48 h post removal of 6-thioG, which becomes much more pronounced at the 72 h time point (Fig. 2 and Supplementary Fig. S2A). Specifically, we observed that the *Rad51d*$^{+/+}$*Mlh1*$^{+/+}$ cells show 30.9 ± 1.1 % of cells in G2/M while *Rad51d*$^{-/-}$*Mlh1*$^{+/+}$ cells show 65.1 ± 4.8 % in G2/M (Fig. 2A and B), which shows that the G2 arrest in MMR proficient cells is heightened by HR deficiency. *Rad51d*$^{-/-}$*Mlh1*$^{-/-}$ cells show no accumulation of cell in a G2/M population, which confirms that functional MMR is necessary for the cell cycle arrest in response to 6-thioG (Fig. 2C). Note there is no observable arrest 24 h following treatment in any of the cell lines used.

To confirm that the arrest was in G2 and determine whether the G2 checkpoint response was altered by the failure to complete HR, the mitotic index of the *Rad51d*$^{-/-}$*Mlh1*$^{+/+}$ and *Rad51d*$^{+/+}$*Mlh1*$^{+/+}$ cells was determined by phospho-histone H3 (Ser 10) staining (Fig. 3). Nocodazole trapping was used to quantify the progression of G2 cells into mitosis. At 48 h, the mitotic index of the *Rad51d*-proficient cells treated with 6-thioG was reduced by 3.6% compared to the untreated cells (Fig. 3A). However at 48 h, the mitotic index of the *Rad51d*-deficient cells was reduced by 5.9% compared to untreated cells (Fig. 3C). In other words, the data demonstrate that 6-thioG treatment induces a G2 arrest, which is more pronounced in the *Rad51d*-deficient cells. At 72 h, the reduction in mitotic index caused by 6-thioG treatment was less than that seen at 48 h in both genotypes. Specifically, the *Rad51d*-proficient cells were reduced by 1.7% while that of the *Rad51d*-deficient cells was reduced by 3.3% (Fig. 3B and D). This data suggests that the G2 arrest does not persist to 72 h and the cells eventually progress into mitosis, although there are dire consequences in the HR-deficient cells (next section). Several conclusions can be drawn from these data. First, it confirms that the initial arrest is G2, not mitotic. Second, the absence of HR in the *Rad51d*-deficient cells heightened the G2 arrest induced by 6-thioG, suggesting that HR intermediates cause the G2 arrest. Third, the HR intermediates are MMR-dependent, i.e., MMR is generating the substrate that activates HR. Fourth, the G2 arrest observed does not depend on RAD51D, because the arrest is heightened in the *Rad51d*-deficient cells.

The cell cycle data also revealed what appeared to be a substantial induction of cells with >4n DNA content, so the number of cells with the >4n DNA content was quantified (Supplementary Fig. S2A). At the 72 h time point, *Rad51d*$^{+/+}$*Mlh1*$^{+/+}$ cells show 1.8-fold

increase in the number of cells with >4n DNA content while *Rad51d*$^{-/-}$*Mlh1*$^{+/+}$ cells show a 3.1-fold induction in the aneuploid population (Fig. 4). *Rad51d*$^{-/-}$*Mlh1*$^{-/-}$ cells did not show an increase in the aneuploid population, confirming the MMR dependence of the damage. The apparent induction of aneuploidy compelled us to examine the nuclear integrity and chromosomal instability in the different genotypes.

6-ThioG induced multinucleation in the absence of HR

We examined the cells by DAPI and β-tubulin staining to directly visualize nuclear integrity. Interestingly, exposure to 6-thioG caused multinucleation in *Rad51d*-proficient and deficient cells in the MMR-proficient background (Fig. 5, see also representative images in Supplementary Fig. S3). The percentages of multinucleated cells were the same in untreated and treated cells at 24 h post treatment, although the basal level of multinucleated cells in the *Rad51d*-deficient cells was 2.3-fold higher ($P < 0.05$). At 48 h, *Rad51d*-proficient cells show a 3.3% increase in multinucleated cells compared to untreated cells, while *Rad51d*-deficient cells show a 7.6% increase. By 72 h, the *Rad51d*-proficient cells show a 6.8% increase while the *Rad51d*-deficient cells show an 18.0% increase in multinucleated cells compared to the untreated cells (Fig. 5A and B). In the MMR-deficient background *Rad51d*-deficient cells show only a 2.0% increase in multinucleated cells compared to the untreated cells, demonstrating the dependence on MMR (Fig. 5C; $P>0.05$).

Increased 6-ThioG induced chromosomal aberrations in the absence of HR

We next examined the influence of HR on chromosomal instability following 6-thioG treatment focusing on MMR proficient cells, because it has been shown that 6-thioG induced chromosome aberrations are not observed in MMR deficient cells (11). In *Rad51d*-proficient cells, there was a 3.1 fold increase in the number of total aberrations 24 h post-treatment and a 3.5 fold increase by 48 h (Fig. 6A). In *Rad51d*-deficient cells there was a 3.5 fold increase 24 h post treatment, but a much larger (9.4 fold) increase at 48 h post treatment (Fig. 6B). The fold-inductions are calculated by comparing the treated samples to the corresponding untreated control for that genotype. It is important to note that *Rad51d*-deficient cells have an approximately 5-fold higher background level of total aberrations, so the 9.4-fold increase seen by 48 h represents an extraordinary level of chromosomal instability induced by the low (0.1 μM) dose of 6-thioG (note different Y-axes in Fig. 6A and B). By 72 h, the fold induction of all chromosomal aberrations seen in the *Rad51d*-deficient cells remained at 9.5, but there was a dramatic increase in the number of complex exchange type aberrations. Of particular note was a huge induction of radials (25-fold) in *Rad51d*-deficient cells treated with 6-thioG, compared to a 1.3-fold induction in the *Rad51d*-proficient cells (Fig. 6C and D). Moreover, there were complex, presumptive interchromosomal intermediates evident only in the *Rad51d*-deficient cells that were not quantified (Examples are shown in Supplementary Fig. S4). Collectively, this data suggests that chromosomal fusions were occurring in the absence of HR.

6-thioguanine has been shown to increase sister chromatid exchanges (SCEs), presumptive HR events, in MMR proficient cells (11). We observed a 1.9-fold increase in SCEs in *Rad51d*-proficient cells after treatment with 0.1 μM 6-thioG. However, there was no detectable increase in SCEs in *Rad51d*-deficient cells, demonstrating that the absence of RAD51D has prevented the induction of SCEs by MMR recognition of 6-thioG (Supplementary Fig. S5), and suggesting that HR is indeed defective in *Rad51d*-deficient cells.

Discussion

Here, we report that *Rad51d*-deficient cells are hypersensitive to 6-thioG, and that this sensitivity is rescued by deletion of *Mlh1*. The observations in this study have several important implications for understanding the role of HR in response to the DNA damage caused by thiopurines. The data clearly places HR downstream of MMR, and also demonstrate an almost exclusive dependence on MMR for the genotoxic effects of thiopurines. It has been demonstrated that 6-thioG induces a G2 arrest in MMR-proficient cells (22). *Rad51d*-deficient cells display more G2 accumulation in response to 6-thioG, suggesting that the G2 checkpoint machinery is intact. However, the G2 arrest was transient and by 72 h both *Rad51d*-deficient and proficient cells show progression into mitosis. HeLa cells exposed to low dose of MNNG have been previously demonstrated to undergo a transient G2 arrest before entering into mitosis (23). Our results show that the status of RAD51D-dependent HR does not affect the activation of the G2 checkpoint or exit from the G2 arrest. However, dramatic chromosomal instability occurs when the HR-deficient cells enter into mitosis following 6-thioG treatment.

The induction of chromosomal aberrations and SCEs in MMR and HR proficient cells provides strong evidence that MMR is causing a direct DNA intermediate that must be resolved by a DSB repair process. In the absence of HR, the chromosomal instability induced by 6-thioG dramatically worsens, and appears to invoke a different DSB process. Recent studies suggest that in HR-deficient cells, alternative end joining pathways tend to join the DNA breaks and produce complex chromosome rearrangements (24). We did not observe an appreciable change in the nuclear localization of two representative NHEJ participants, Ku70 and XRCC4, (data not shown), which implies that classical NHEJ is not responsible. However, we did see a statistically significant increase in XRCC1 foci at 72 h (data not shown), which was the same time point at which the radial induction occurred (Figure 6). This suggests that an alternative NHEJ pathway is likely triggering the observed fusion events in the absence of RAD51D. The basis of the alternative NHEJ process that results in the formation of radials remains under active investigation.

6-thioG treatment induces centrosome amplification in MMR-proficient cells, which gives rise to aneuploid and multinucleated cells (25). *Rad51d*-deficient cells also displayed an increase in the aneuploid population and multinucleated cells in response to 6-thioG. Aneuploidy and multinucleation are associated with various leukemias and lymphomas, for example, a cell type associated with the pathology of Hodgkin's lymphoma known as Reed-Sternberg (RS) cells, which coincidently are MMR proficient (26). RS cells are giant multinucleated cells that display hyperdiploid DNA content, and the DNA is unequally partitioned among the nuclei. RS cells also show telomere dysfunction and centrosome amplification (27,28). Coincidently, we have shown that telomere dysfunction and centrosome amplification are associated with *Rad51d*-deficiency (19,29). It is therefore tempting to speculate that RAD51D insufficiency can drive telomere and chromosomal instability associated with the progression of Hodgkin's cells to RS cells. Recently, XRCC2 (another Rad51-parolog and also part of a protein complex that includes RAD51D) has been implicated in B-cell development (30). Specifically, the study directly implicated XRCC2 in suppressing genomic instability in B-cells caused by activation induced cytidine deaminase. This paper strongly suggests that RAD51-dependent HR is required to suppress the development of B-cell lymphomas. We believe the tumor suppressing activity of RAD51-dependent HR more broadly extends to therapy-induced malignancies.

A large number of Hodgkin's lymphoma patients develop secondary tumors after chemotherapy (31,32). Therefore, HR-insufficiency could be risk factor for Hodgkin's and an additional important consideration of treatment options for these patients because HR

status may predispose these patients to the development of secondary cancers resulting from chemotherapy treatment. Although many patients have benefited from thiopurines, there is growing concern for long term survivors of an increased risk of iatrogenic (therapy-induced) cancer. While this manuscript was in preparation, a study reported that BRCA2-deficient cells are sensitized to 6-thioG (17), which agrees with the findings here in *Rad51d*-deficient cells. One implication is that HR defective tumors might be successfully treated with thiopurines. However, there are a number of important caveats that might suggest healthy caution before treating BRCA2 carriers with thiopurines. First, the chromosomal instability induced by 6-thioG treatment in the HR-defective cells was impressive in its extent and complexity. The chromosomal instability observed is highly likely to result from unresolved HR intermediates, and the outcomes appear to be chromosomal fusions. The fact that MMR proficiency promotes cell death following thiopurine treatment sets up a strong selection pressure for loss of MMR, certainly *in vitro* (33). In fact, it has observed that although microsatellite instability (MSI) associated with MMR deficiency is not associated with the development of de novo hematological malignancies, the frequency of MMR defects in therapy related leukemia is high (34). *Mlh1* polymorphism has been associated with an increased risk of secondary cancers in Hodgkin's lymphoma patients after methylating chemotherapy (32). This suggests that thiopurine treatment indeed puts a selection for the outgrowth of MMR-defective cells in patients. There is a possibility that HR insufficiency will not only play a role increasing the selection pressure on these cells to select for MMR-deficiency but also play an important role during the progression of MSI-positive lymphomas by increasing the overall chromosome instability characterizing these cancers. This provides indirect evidence that proficiency in MMR and insufficiencies in HR might predispose such patients for thiopurine-induced leukemias and lymphomas. It also suggests that variations in HR capacity might explain susceptibility to thiopurine-induced cancer.

Supplementary Material

Refer to Web version on PubMed Central for supplementary material.

Acknowledgments

Grant Support: This research was supported in part by a grant from the NIH to the Center for Colon Cancer Research at USC (P20 RR17698), from the NIH/NCI to MDW (R01 CA100450) and from the American Cancer Society to DLP (RSG-03-158-01-GMC).

References

1. Karran P. Thiopurines, DNA damage, DNA repair and therapy-related cancer. Br Med Bull 2006;79-80:153–70. [PubMed: 17277075]
2. Beaugerie L, Brousse N, Bouvier AM, et al. Lymphoproliferative disorders in patients receiving thiopurines for inflammatory bowel disease: a prospective observational cohort study. Lancet 2009;374(9701):1617–25. [PubMed: 19837455]
3. Schmiegelow K, Al-Modhwahi I, Andersen MK, et al. Methotrexate/6-mercaptopurine maintenance therapy influences the risk of a second malignant neoplasm after childhood acute lymphoblastic leukemia: results from the NOPHO ALL-92 study. Blood 2009;113(24):6077–84. [PubMed: 19224761]
4. Klapacz J, Meira LB, Luchetti DG, et al. O6-methylguanine-induced cell death involves exonuclease 1 as well as DNA mismatch recognition in vivo. Proc Natl Acad Sci U S A 2009;106(2):576–81. [PubMed: 19124772]
5. Schaetzlein S, Kodandaramireddy NR, Ju Z, et al. Exonuclease-1 deletion impairs DNA damage signaling and prolongs lifespan of telomere-dysfunctional mice. Cell 2007;130(5):863–77. [PubMed: 17803909]

6. Karran P. Mechanisms of tolerance to DNA damaging therapeutic drugs. Carcinogenesis 2001;22(12):1931–7. [PubMed: 11751422]
7. O'Brien V, Brown R. Signalling cell cycle arrest and cell death through the MMR System. Carcinogenesis 2006;27(4):682–92. [PubMed: 16332722]
8. Stojic L, Brun R, Jiricny J. Mismatch repair and DNA damage signalling. DNA Repair (Amst) 2004;3(8-9):1091–101. [PubMed: 15279797]
9. Lin DP, Wang Y, Scherer SJ, et al. An Msh2 point mutation uncouples DNA mismatch repair and apoptosis. Cancer Res 2004;64(2):517–22. [PubMed: 14744764]
10. Yang G, Scherer SJ, Shell SS, et al. Dominant effects of an Msh6 missense mutation on DNA repair and cancer susceptibility. Cancer Cell 2004;6(2):139–50. [PubMed: 15324697]
11. Armstrong MJ, Galloway SM. Mismatch repair provokes chromosome aberrations in hamster cells treated with methylating agents or 6-thioguanine, but not with ethylating agents. Mutat Res 1997;373(2):167–78. [PubMed: 9042397]
12. Rajesh P, Rajesh C, Wyatt MD, Pittman DL. RAD51D protects against MLH1-dependent cytotoxic responses to O(6)-methylguanine. DNA Repair (Amst) 2010;9(4):458–67. [PubMed: 20133210]
13. Rajesh C, Gruver AM, Basrur V, Pittman DL. The interaction profile of homologous recombination repair proteins RAD51C, RAD51D and XRCC2 as determined by proteomic analysis. Proteomics 2009;9(16):4071–86. [PubMed: 19658102]
14. Mojas N, Lopes M, Jiricny J. Mismatch repair-dependent processing of methylation damage gives rise to persistent single-stranded gaps in newly replicated DNA. Genes Dev 2007;21(24):3342–55. [PubMed: 18079180]
15. Roos WP, Nikolova T, Quiros S, et al. Brca2/Xrcc2 dependent HR, but not NHEJ, is required for protection against O(6)-methylguanine triggered apoptosis, DSBs and chromosomal aberrations by a process leading to SCEs. DNA Repair (Amst) 2009;8(1):72–86. [PubMed: 18840549]
16. Tebbs RS, Hinz JM, Yamada NA, et al. New insights into the Fanconi anemia pathway from an isogenic FancG hamster CHO mutant. DNA Repair (Amst) 2005;4(1):11–22. [PubMed: 15533833]
17. Issaeva N, Thomas HD, Djurenovic T, et al. 6-Thioguanine Selectively Kills BRCA2-Defective Tumors and Overcomes PARP Inhibitor Resistance. Cancer Research 2010;70(15):6268–76. [PubMed: 20631063]
18. Tate EH, Wilder ME, Cram LS, Wharton W. A method for staining 3T3 cell nuclei with propidium iodide in hypotonic solution. Cytometry 1983;4(3):211–5. [PubMed: 6198128]
19. Smiraldo PG, Gruver AM, Osborn JC, Pittman DL. Extensive chromosomal instability in Rad51d-deficient mouse cells. Cancer Res 2005;65(6):2089–96. [PubMed: 15781618]
20. Buermeyer AB, Wilson-Van Patten C, Baker SM, Liskay RM. The human MLH1 cDNA complements DNA mismatch repair defects in Mlh1-deficient mouse embryonic fibroblasts. Cancer Res 1999;59(3):538–41. [PubMed: 9973196]
21. Yamane K, Schupp JE, Kinsella TJ. BRCA1 activates a G2-M cell cycle checkpoint following 6-thioguanine-induced DNA mismatch damage. Cancer Res 2007;67(13):6286–92. [PubMed: 17616687]
22. Yan T, Desai AB, Jacobberger JW, Sramkoski RM, Loh T, Kinsella TJ. CHK1 and CHK2 are differentially involved in mismatch repair-mediated 6-thioguanine-induced cell cycle checkpoint responses. Mol Cancer Ther 2004;3(9):1147–57. [PubMed: 15367709]
23. Schroering AG, Kothandapani A, Patrick SM, Kaliyaperumal S, Sharma VP, Williams KJ. Prolonged cell cycle response of HeLa cells to low-level alkylation exposure. Cancer Res 2009;69(15):6307–14. [PubMed: 19638578]
24. Bunting SF, Callen E, Wong N, et al. 53BP1 inhibits homologous recombination in Brca1-deficient cells by blocking resection of DNA breaks. Cell 2010;141(2):243–54. [PubMed: 20362325]
25. Robinson HM, Black EJ, Brown R, Gillespie DA. DNA mismatch repair and Chk1-dependent centrosome amplification in response to DNA alkylation damage. Cell Cycle 2007;6(8):982–92. [PubMed: 17404511]

26. Re D, Benenson L, Wickenhauser C, et al. Proficient mismatch repair protein expression in Hodgkin and Reed Sternberg cells. Int J Cancer 2002;97(2):205–10. [PubMed: 11774265]
27. Knecht H, Sawan B, Lichtensztejn D, Lemieux B, Wellinger RJ, Mai S. The 3D nuclear organization of telomeres marks the transition from Hodgkin to Reed-Sternberg cells. Leukemia 2009;23(3):565–73. [PubMed: 19039323]
28. Martin-Subero JI, Knippschild U, Harder L, et al. Segmental chromosomal aberrations and centrosome amplifications: pathogenetic mechanisms in Hodgkin and Reed-Sternberg cells of classical Hodgkin's lymphoma? Leukemia 2003;17(11):2214–9. [PubMed: 14523479]
29. Tarsounas M, Munoz P, Claas A, et al. Telomere maintenance requires the RAD51D recombination/repair protein. Cell 2004;117(3):337–47. [PubMed: 15109494]
30. Hasham MG, Donghia NM, Coffey E, et al. Widespread genomic breaks generated by activation-induced cytidine deaminase are prevented by homologous recombination. Nat Immunol 2010;11(9):820–6. [PubMed: 20657597]
31. Allan JM, Travis LB. Mechanisms of therapy-related carcinogenesis. Nat Rev Cancer 2005;5(12): 943–55. [PubMed: 16294218]
32. Worrillow LJ, Smith AG, Scott K, et al. Polymorphic MLH1 and risk of cancer after methylating chemotherapy for Hodgkin lymphoma. J Med Genet 2008;45(3):142–6. [PubMed: 17959715]
33. Karran P, Offman J, Bignami M. Human mismatch repair, drug-induced DNA damage, and secondary cancer. Biochimie 2003;85(11):1149–60. [PubMed: 14726020]
34. Karran P, Attard N. Thiopurines in current medical practice: molecular mechanisms and contributions to therapy-related cancer. Nat Rev Cancer 2008;8(1):24–36. [PubMed: 18097462]

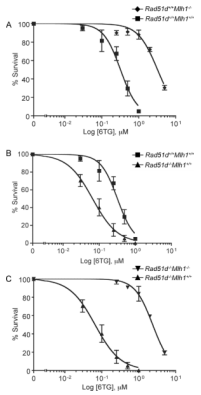

Figure 1. Rad51d-deficient MEFs are extremely sensitive to 6-thioG in an MMR-proficient background

Colony survival assays of MEFs deficient in *Rad51d*, *Mlh1* or both, treated with 6-thioG at the indicated doses. (A) Pair wise comparison of *Mlh1*-deficient (◆) and *Mlh1*-proficient (■) MEFs. (B) Pair wise comparison of *Rad51d*-proficient (■) and *Rad51*-deficient MEFs (▲). (C) Pair wise comparison of *Rad51d*-deficient *Mlh1*-proficient (▲) and *Rad51d*-deficient *Mlh1*-deficient (▼) MEFs. Survival is plotted as percentage compared to untreated control. Each data point represents the mean of three independent experiments each performed in triplicate. Error bars represent the standard error of means.

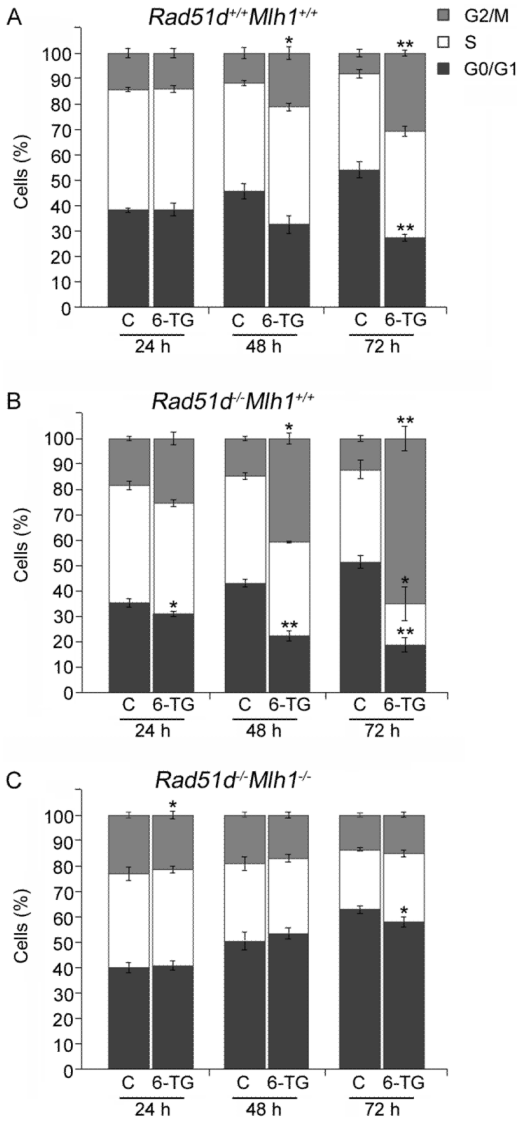

Figure 2. Cell cycle progression of Rad51d-deficient and proficient MEFs in response to 6-thioG in Mlh1-proficient and deficient backgrounds

Cell cycle progression was followed for untreated cells and those treated with 0.1 μM 6-thioG for 6 h. Percentage of the cells in the G1, S and G2/M phases in the diploid population were calculated using MODFIT-LT software and shown for (A) *Rad51d*$^{+/+}$*Mlh1*$^{+/+}$, (B) *Rad51d*$^{-/-}$*Mlh1*$^{+/+}$ and (C) *Rad51d*$^{-/-}$*Mlh1*$^{-/-}$. Each data point represents the mean of three independent experiments. Error bars represent the standard error of means. Statistical significance was determined by paired t-test (* P<0.05; ** P<0.01).

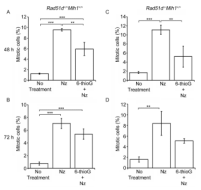

Figure 3. Rad51d-deficient cells display a G2 arrest after treatment with 6-thioG

Following 6 h treatment with 0.1 μM 6-thioG, the cells were harvested at the 48 h and 72 h time-points post treatment for *Rad51d*-proficient cells (A, B) and *Rad51d*-deficient cells (C, D). Nocodazole was added 6 h prior to harvesting the cells and the mitotic index was calculated. Each data point represents the mean of three independent experiments. Error bars represent the standard error of means. Statistical significance was determined by ANOVA followed by Bonferroni's multiple comparison's test (** P<0.01; *** P<0.001).

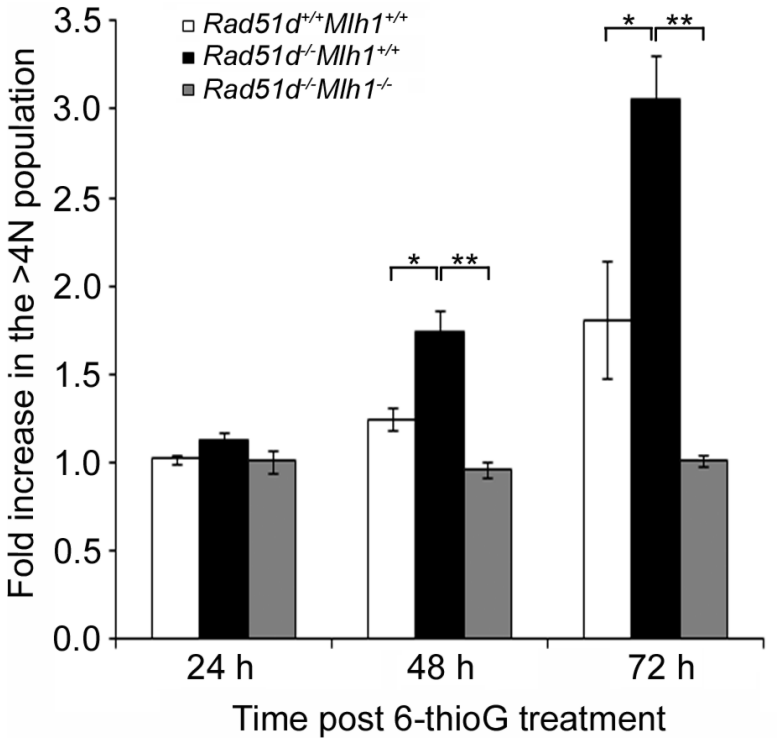

Figure 4. 6-thioG induces the appearance of cells with >4n DNA content in Rad51d-deficient cells

Rad51d$^{+/+}$*Mlh1*$^{+/+}$, *Rad51d*$^{-/-}$*Mlh1*$^{+/+}$ and *Rad51d*$^{-/-}$*Mlh1*$^{-/-}$ cells were treated with 0.1 μM 6-thioG for 6 h. Cells were harvested at 24 h, 48 h and 72 h post treatment. The number of cells containing >4n DNA content were quantified using the MODFIT-LT software, and fold induction was calculated by normalizing the data of the treated population to that of the untreated controls. The data represents the mean of three independent experiments. Error bars represent the standard error of means. Statistical significance was determined by ANOVA followed by Bonferroni's multiple comparison's test (* $P<0.05$; ** $P<0.01$).

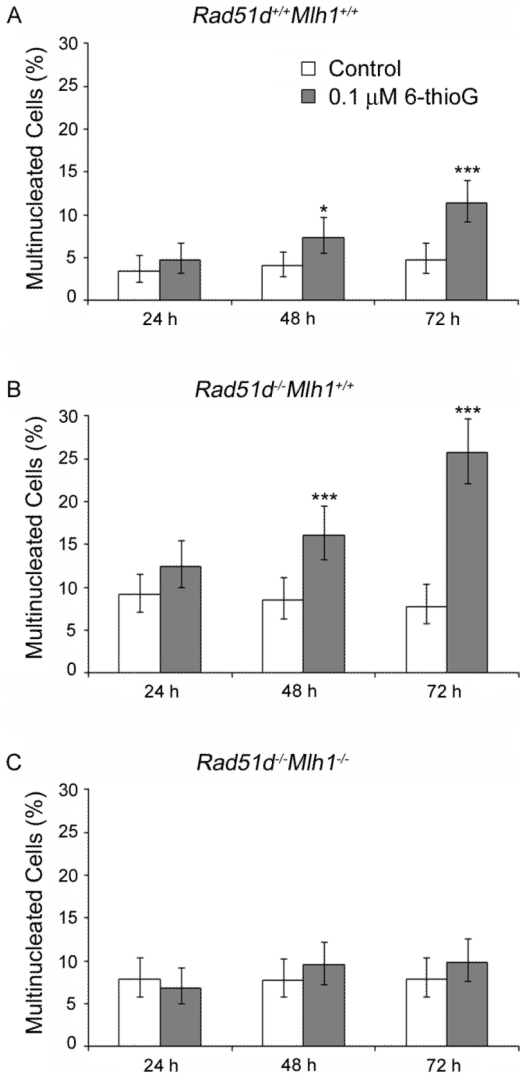

Figure 5. 6-thioG treatment induces increased multinucleation in Mlh1-proficient and Rad51d-deficient cells

(A) *Rad51d*$^{+/+}$*Mlh1*$^{+/+}$, (B) *Rad51d*$^{-/-}$*Mlh1*$^{+/+}$ and (C) *Rad51d*$^{-/-}$*Mlh1*$^{-/-}$ cells were treated with 0.1 μM 6-thioG for 6 h and harvested at 24 h, 48 h and 72 h post treatment. Percentages of multinucleated cells were calculated from at least 500 cells per sample. Error bars represent the 95% confidence intervals. Statistical significance was determined by z-test (* P<0.05; *** P<0.001).

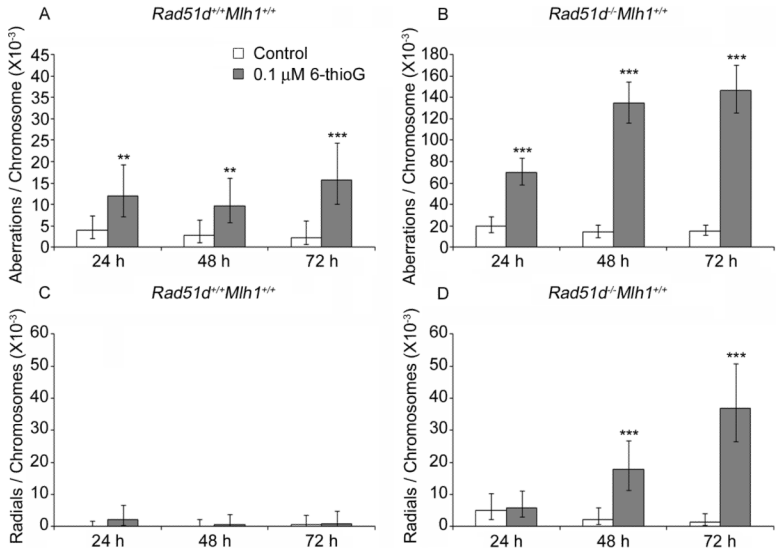

Figure 6. Rad51d-deficient cells display increased chromosomal instability after 6-thioG treatment

Total number of aberrations (gaps, breaks, tri-, quadriradials, fusions and giant marker chromosomes) per chromosome × 10^{-3} as detected by Giemsa staining of metaphase spreads from (A) *Rad51d*$^{+/+}$*Mlh1*$^{+/+}$ and (B) *Rad51d*$^{-/-}$*Mlh1*$^{+/+}$ MEF cell lines treated with 0.1 μM 6-TG for 6 h. The aberration frequencies were calculated 24 h, 48 h, and 72 h post-treatment. Note different Y-axis scales. Triradial and Quadriradial aberrations per chromosome × 10^{-3} as detected by Giemsa staining of metaphase spreads from (C) *Rad51d*-proficient and (D) *Rad51d*-deficient MEF cell lines. Error bars represent the 95% confidence intervals. Statistical significance was determined by z-test (** P<0.01; *** P<0.001).